Spine

SPINE Volume 47, Number 16, pp 1172–1178

BASIC SCIENCE

OPEN

Novel Pedicle Navigator Based on Micro Inertial Navigation System (MINS) and Bioelectric Impedance Analysis (BIA) to Facilitate Pedicle Screw Placement in Spine Surgery: Study in a Porcine Model

Wentao Lin,[a] Faqin Xie,[a] Shuofeng Zhao,[b] Songhui Lin,[a] Chaoqin He,[a] and Zhiyun Wang, MD[a]

Study Design. A porcine model.

Objective. The study aims to design a novel pedicle navigator based on micro-inertial navigation system (MINS) and bioelectrical impedance analysis (BIA) to assist place pedicle screw placement and validate the utility of the system in enhancing pedicle screw placement.

Summary of Background Data. The incidence of pedicle screw malpositioning in complicated spinal surgery is still high. Procedures such as computed tomography image-guided navigation, and robot-assisted surgery have been used to improve the precision of pedicle screw placement, but it remains an unmet clinical need.

Methods. The miniaturized integrated framework containing MINS was mounted inside the hollow handle of the pedicle finder. The inner core was complemented by a high-intensity electrode for measuring bioelectric impedance. Twelve healthy male Wuzhishan minipigs of similar age and weight were used in this experiment and randomized to the MINS-BIA or freehand (FH) group. Pedicle screw placement was determined according to the modified Gertzbein–Robbins grading system on computed tomography images. An impedance detected by probe equal to the baseline value for soft tissue was defined as cortical bone perforation.

Results. A total of 216 screws were placed in 12 minipigs. There were 15 pedicle breaches in the navigator group and 31 in the FH group; the detection rates of these breaches were 14 of 15 (93.3%) and 25 of 31 (80.6%), respectively, with a statistically significant difference between groups. The mean offsets between the planned and postoperatively measured tilt angles of the screw trajectory were 4.5° ± 5.5° in the axial plane and 4.8° ± 3.3° in the sagittal plane with the navigator system and 7.0° ± 5.1° and 7.7° ± 4.7°, respectively, with the FH technique; the differences were statistically significant.

Conclusion. A novel and portable navigator based on MINS and BIA could be beneficial for improving or maintaining accuracy while reducing overall radiation exposure.

Key words: bioelectrical impedance analysis, internal fixation, micro inertial navigation system, navigation surgery, pedicle screw.

Spine 2022;47:1172–1178

From the [a]Department of Spine Surgery, Shunde Hospital, Southern Medical University (The First People's Hospital of Shunde Foshan), Foshan, Guangdong, china; and [b] School of Ophthalmology and Optometry, School of Biomedical Engineering, Wenzhou Medical University, Wenzhou, Zhejiang China.

Acknowledgment date: September 19, 2021. First revision date: February 8, 2022. Acceptance date: February 8, 2022.

W.L. and F.X. contributed equally to this work.

Source of Funding: Z.W. has received funding from the Foundation of Science and Technology Program of Guangzhou (201704020156), Guangdong Basic and Applied Basic Research Foundation (2021A1515011508), and Open Research Fund of State Key Laboratory of Bioelectronics, Southeast University (Sklb2021-k04); W.L. has received funding from the Scientific Research Start Plan of Shunde Hospital, Southern Medical University (SRSP2021007).

Ethical review committee statement: The study was performed in accordance with the ethical standards in the 1964 Declaration of Helsinki. The protocol was approved by the institutional Animal Experimental Ethics Committee of the General Hospital of Southern Theater Command (IRB: 2020102202).

Guangzhou Asensing Technology Co., Ltd provided general guidance on functional debugging, and Guangzhou Aquila Precise Tools Ltd provided hardware assembly guidance.

Address correspondence and reprint requests to Zhiyun Wang, MD, Chairman of the Department of Spine Surgery, Shunde Hospital, Southern Medical University, No.1 Jiazi Rd, Shunde District, Foshan City, Guangdong Province 528308, China; E-mail: dragon201@126.com.

DOI: 10.1097/BRS.0000000000004348

In 1959, Boucher first applied pedicle screw instrumentation to lumbar fusion surgery.[1] Because of its high mechanical stability by three-column fixation, the

procedure has been widely adopted for internal fixation of the spine in recent years.[2,3] However, it is still clinically challenging: the pedicle screw malpositioning rate in complicated spinal surgery, such as posterior cervical spine surgery and adolescent scoliosis orthopedic surgery, ranges from 11.2% to 33%.[4–6] Because of the proximity to the spinal canal and surrounding vessels, misplacement of the pedicle screw can lead to various complications.

Procedures such as x-ray fluoroscopy, computed tomography (CT) image-guided navigation, and robot-assisted surgery are increasingly being used to improve the precision of pedicle screw placement.[7–9] However, these methods have various limitations, including large volume, high cost, radiation exposure, and cumbersome and complex operation,[10] and thus fail to meet clinical needs. As such, a simple and low-cost technique that can monitor screw trajectory in real-time is needed.

The self-contained micro inertial navigation system (MINS) provides information on the carrier's attitude, velocity, and position. MINS is widely used in automobiles, aircraft, missiles, and robots because of its high autonomy and reliability.[11,12] Using MINS, a surgeon can determine real-time axial and sagittal tilt angles of implanted screws from the data provided by the inertial measurement unit (IMU). The IMU used for MINS includes a three-axis gyroscope, accelerometer, and magnetometer, usually mounted on the body directly. The three-axis gyroscope and accelerometer measure the object's linear and angular acceleration along the x, y, and z axes, to obtain the three degrees of freedom of the pedicle instrument at arbitrary positions by collecting positional information with six degrees of freedom from three orthogonal-sensing axes. A computer algorithm is used to solve the inertial data to calculate tilt angles in the axial and sagittal planes.[13] The magnetometer is able to calibrate gyroscope drift and increase measurement sensitivity by measuring the direction and intensity of the magnetic field.[14]

Bioelectric impedance analysis (BIA) is an inexpensive, easy to perform, and radiation-free technique for measuring body composition based on the relationship between total body impedance and total body water.[15] Iatrogenic cortical bone perforation is detected by measuring impedance changes when the instrument traverses the boundary between two different media—namely, cortical bone and soft tissue.

Considering the advantages of BIA and MINS, the present study had the following aims: to design a portable, inexpensive, stable, easy to use, and radiation-free navigation system for the accurate placement of pedicle screws based on these techniques; to validate the utility of the system in enhancing pedicle screw placement in an animal model.

MATERIALS AND METHODS

Integrated Pedicle Finder Design

A 169-mm-long hollow cylinder shell with an external diameter of 3 mm and an internal diameter of 2 mm was fabricated by high-precision computer-controlled machining, and the design of the navigator tip was developed with a tilt angle of 30°. The shell was complemented by a high-intensity electrode for measuring bioelectric impedance (BI). A small amount of polyether ether ketone film was evenly spread over the electrode as a 50-μm insulator layer. The total length of the navigator was 269 mm (Figure 1). The miniaturized integrated framework was mounted inside the pedicle instrument to enable intraoperative monitoring of angle changes in real-time.

Building a Visualization Interface

Data collected by the built-in electrode and sensors were wirelessly transmitted via Bluetooth to a personal computer. Data pertaining to the BI of body tissue and angle information of the pedicle instrument were viewed on the computer using software that was designed in-house (Figure 2).

Animal Experiments

This study was approved by the institutional Animal Experimental Ethics Committee (No. 2020102202). Healthy male Wuzhishan minipigs (n = 12) of similar age (4–6 months) and weight (10–12.5 kg) were used in this experiment and randomized to the MINS-BIA or free-hand (FH) group. All pigs underwent CT scans before surgery, and the screw trajectory was selected based on 3D-reconstructed images. All surgical procedures were performed by the same spine surgeon.

After general anesthesia, an incision was made over the mid-lumbar region, and then the spinous process, lamina, and articular processes were exposed. Screws were implanted into bilateral pedicles using the portable navigator

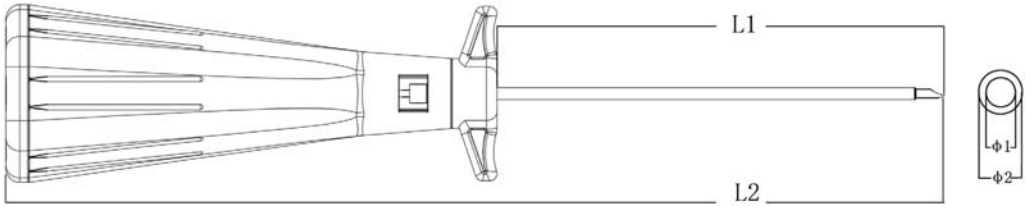

Figure 1. A much more detailed model of the pedicle finder. L1: hollow cylinder shell length; L2: total length; Φ1: internal diameter; Φ2: external diameter.

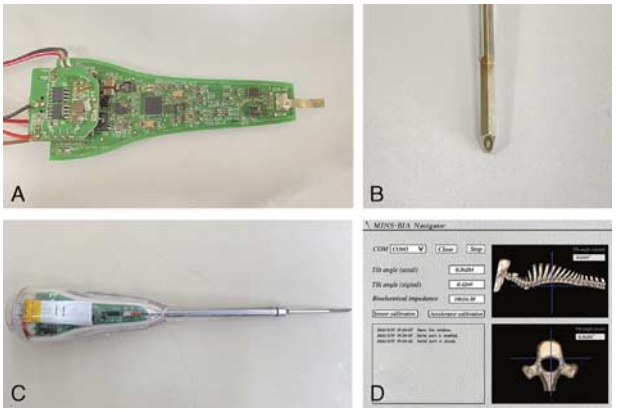

Figure 2. Composition of the MINS-BIA navigator. (A) A integrated hardware framework based on MINS. (B) The conductive electrode was built into the tip of the pedicle navigator. (C) Assembled device combine with integrated hard ware and conductive electrode. (D) A visualization interface. full color online

in the MINS-BIA group and an FH technique in the FH group. The screw trajectory and BI values were measured and recorded during the surgery. The minipigs underwent another CT scan after they were sacrificed. Pedicle screw trajectory and angulation were measured in the 3D-reconstructed images, and cortical bone breaches were analyzed in the axial and sagittal planes.

Pedicle screw placement consists of three significant steps: identifying the optimal entry point (positioning), correctly inserting the screw (orientation), and measuring vertebral cortical integrity (qualitative evaluation). First, a zero or reference orientation was set for the MINS: one line was along the ventrodorsal axis of the spinous process, and the other was perpendicular to the supraspinous ligament. For positioning, 3D CT image reconstruction was performed to obtain detailed stereoscopic images of spinal anatomy that aided the preoperative determination of the

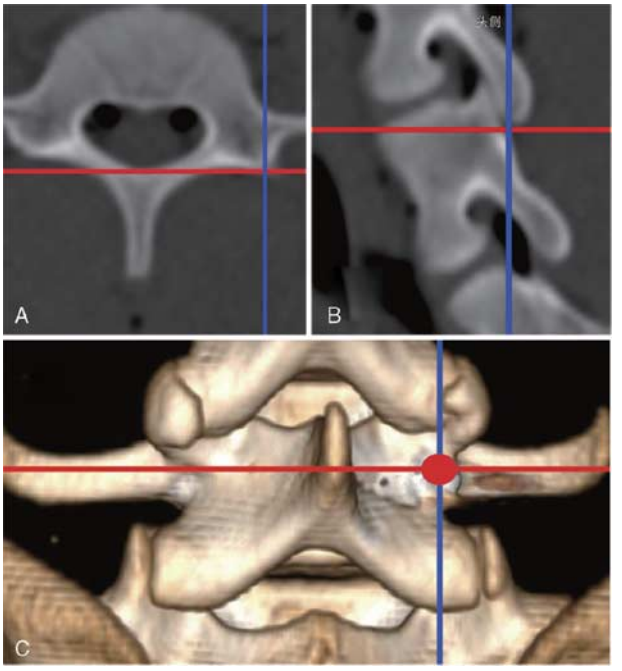

Figure 3. Identifying the optimal entry point. The start site of screw trajectories was depicted in the axial (A) and sagittal views (B), respectively. (C) The optimal entry point of pedicle screw was identifying on 3D rendered spinal anatomy. full color online

entry point. Preoperative 2D images were first examined to identify the desired screw trajectory in the sagittal and axial planes at the surgical level (Figure 3A and 3B), and then switched to a 3D-rendered view of the spine to preset the entry point of the pedicle screw (Figure 3C) at the intersection of the two planes. The planned entry point was intraoperatively selected by the surgeon and corresponding anatomic structures were identified. For the orientation in the MINS-BIA group, the pedicle finder was first oriented along the craniocaudal axis of the spine to set

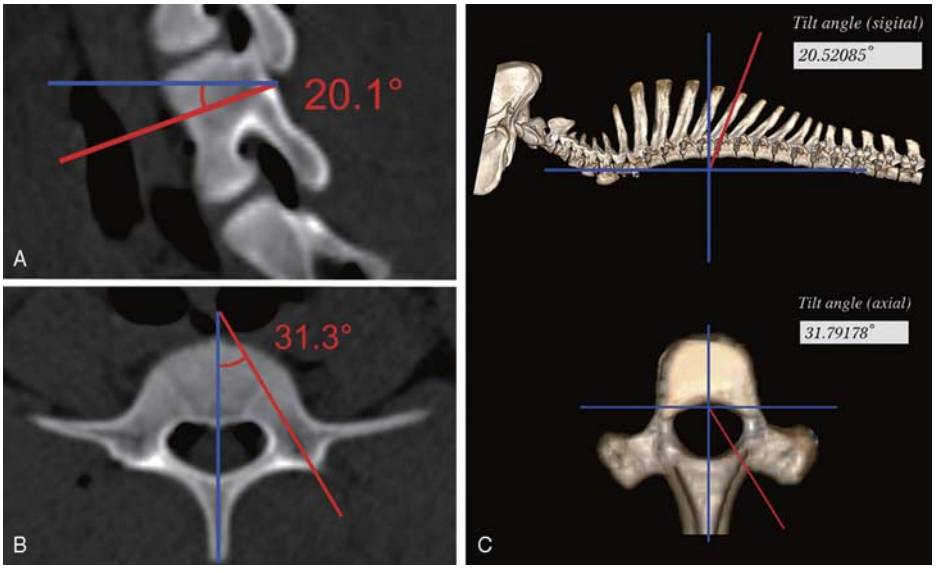

Figure 4. Pre-operative planning of screw trajectory. (A) A planned tilt angle of 20.1° in the sagittal view of preoperative CT. (B) A planned tilt angle of 31.3° in the axial view of preoperative CT. (C) The real-time angle of pedicle navigator was captured by MINS and then visualized on computer interface. full color online

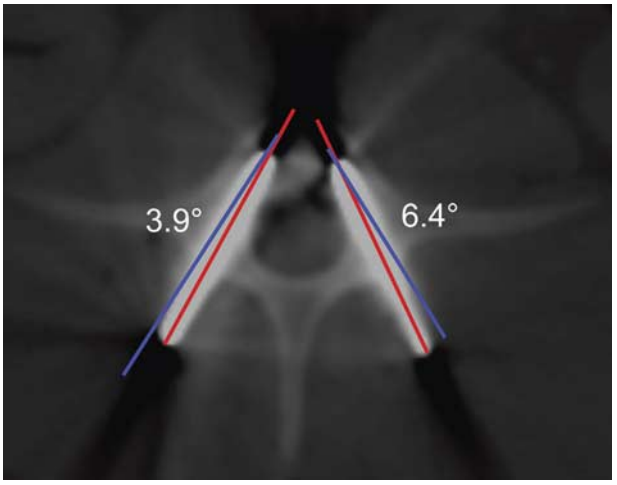

Figure 5. Measurement of deviation angle. The red line represented real screw trajectory, while blue line represented planned screw trajectory. The accuracy of the placement of pedicle screw was evaluated by measuring the angle between the two lines. full color online

the IMU to zero before screw channel preparation and then placed at the predetermined entry point. The orientation of the pedicle finder was slowly adjusted on the screen until it aligned with the planned sagittal and axial tilts (Figure 4). As the instrument was inserted, actual IMU readings of the tilt angles in the sagittal and axial planes were continually registered. To mitigate the risk of cortical perforation because of screw insertion, a Kirschner wire was used in place of a screw and inserted into the pedicle in this experiment. Qualitative evaluation detected the presence/absence of pedicle breach. The essential technique used in the study to facilitate screw placement was real-time monitoring of BI using an electrode mounted on the tip of the pedicle finder.

Pedicle Screw Evaluation

Pedicle screw placement was determined according to the modified Gertzbein–Robbins grading system from the sagittal and axial planes of 3D-reconstructed CT images.[16] Based on previous reports and authors' clinical experience, grades 1 and 2 were considered acceptable screw placements. The correspondence between the planned screw trajectory and actual screw placement was investigated. Briefly, the planes were oriented in the axial and sagittal views of preoperative CT images to display the planned screw trajectory. The actual trajectory of the implanted pedicle screws was determined by the multiplanar reformation mode of 3D reconstruction of postoperative CT images.[17] Another radiologist blinded to the study measured and compared the offsets between planned and actual tilt angles of the screw trajectories in the axial and sagittal planes (Figure 5).

BIA

The detection efficiency was assessed by an investigator unfamiliar with the study in a blinded fashion. The preliminary experiment in a porcine model showed that the baseline BI of soft tissue, cancellous bone, and cortical bone ranged from 2500 to 3300, 4500 to 5500, and >5500 Ω, respectively. In this study, an impedance equal to the baseline value for soft tissue was defined as cortical bone perforation, that is, the pedicle instrument ruptured the cortex as the probe was inserted into the vertebral body. The accuracy of BIA and the FH technique in detecting an impending breach were evaluated by calculation of relevant parameters.[18]

TABLE 1. Results of Cortical Bone Breaches Detected by Different Methods

	MINS-BIA Group	FH Group
Detected by instrument	14	25
Detected by CT	15	31
Sensitivity*	93.3%	80.6%
Specificity†	96.8%	93.5%
Positive predictive value‡	82.3%	83.3%
Negative predictive value§	98.9%	92.3%

CT indicates computed tomography; FH, free-hand; MINS-BIA, micro-inertial navigation system and bioelectrical impedance analysis.

**Probability of detection if there is a breach.*

†Probability of no-detection if there is no breach.

‡Probability of a breach if detection occurred.

§Probability of no breach if no detection occurred.

Statistical Analysis

Measurement data are expressed as mean ± standard deviation, and numerical data are expressed as a percentage. The χ^2 test (Fisher exact probability method) and an independent sample t test were used for statistical analyses. All tests of significance were two-sided, with an alpha of 0.05. Data were analyzed using SPSS v25.0 software (IBM, Armonk, NY).

TABLE 2. Offsets of Screw Trajectory

	MINS-BIA Group	FH Group	*P*
Minipig, n	12	12	—
Total screw, n	108	108	—
Lateral angle†	4.5° ± 2.8°	7.0° ± 5.1°	<0.01*
Cephalad angle‡	4.8° ± 3.3°	7.7° ± 4.7°	<0.01*

FH indicates free-hand; MINS-BIA, micro-inertial navigation system and bioelectrical impedance analysis.

**The data were expressed as mean ± standard deviation, $P < 0.05$.*

†Tilt angle in the axial view.

‡Tilt angle in the sagittal view.

RESULTS

A total of 216 screws were placed in 12 minipigs (108 screws per group). There were 15 pedicle breaches in the navigator group and 31 in the FH group; the detection rates of these breaches were 14 of 15 (93.3%) and 25 of 31 (80.6%), respectively, with a statistically significant difference between groups ($P < 0.01$) (Table 1).

The average distance between the planned entry point in the preoperative CT and the actual entry point in the postoperative CT was 2 mm. The mean offsets between the planned and postoperatively measured tilt angles of the screw trajectory were 4.5° ± 5.5° in the axial plane and 4.8° ± 3.3° in the sagittal plane with the navigator system and 7.0° ± 5.1° and 7.7° ± 4.7°, respectively, with the FH technique; the differences between the two groups were statistically significant ($P < 0.01$) (Table 2).

The sensitivity and specificity of pedicle navigation to detect an impending breach were 93.3% and 96.8%, respectively; the negative and positive predictive values were 98.9% and 82.3%, respectively. With the FH technique, the sensitivity and specificity were 80.6% and 93.5%, respectively, and the negative and positive predictive values were 92.3% and 83.3%, respectively (Table 1).

DISCUSSION

With the development of endoscopic instruments and advances in surgical techniques, spinal surgery has changed from the traditional open approach to minimally invasive and precise procedures. The safety and accuracy of pedicle screw implantation are critical in spinal surgery.[19,20] This study reports a novel and portable pedicle navigator based on MINS and BIA techniques to facilitate pedicle screw placement in a porcine spine model.

In performing a 3D-positioning procedure, there were still 2-mm errors of the entry point between the experimental result and preoperative planning. It was clinically acceptable because the breach rate may not have increased as a result of a 2-mm malpositioning of the entry point. Similar results were reported in a cadaver study that used intraoperative 3D/2D visualization of the spine to select the entry point of the pedicle screw.[21] Visualizing the 3D reconstruction of the spine surface and underlying pedicle and vertebral body in the 2D view may give the surgeon more confidence in the screw placement. However, other studies using an unvarying entry point and sagittal orientation at all levels for thoracic pedicle screw placement have achieved ideal clinical results, demonstrating that it is feasible and safe to implant pedicle screws according to programmed operating steps.[22,23] The above-mentioned method cannot be used in patients with severe spinal deformity because pedicle rotation and wedging often occur in these cases. It was unreliable to place screws at the same entry point. In such situations, CT image reconstruction can be used to establish individualized entry points for pedicle screws, thus increasing the accuracy of screw placement and decreasing the risk of screw malpositioning.[24,25]

The planned screw trajectory was more closely matched under MINS guidance than with the FH technique in both planes. Data from MINS can be used to obtain the attitude and position of the navigator in real-time, and tilt angles were generated algorithmically in a 3D coordinate system. The theoretical orientation precision was $<1°$,[26,27] which is significantly superior to those attained in the present study. The continuous force exerted by the navigator finder during screw channel preparation enabled vertebral body rotation with finder,[28] whereas the initial state with no vertebral rotation was still used as the reference frame for the guided system. It is undeniable that mechanisms of this kind may well contribute to a non-negligible deviation of the tilt angle. In addition, movement of the reference frame as a result of breathing motions or muscle traction can also give inaccurate information. As a result, the accuracy and stability of attitude and position obtained by IMU can be adversely affected. Nonetheless, it is still clinically acceptable to perform a screw trajectory deviation within 5°.[29] Conversely, the FH technique relies on surgeons' eye-hand movements and does not provide objective data to monitor the real-time screw trajectory, which results in a significantly greater angular displacement than the MINS technique. Similar results have been reported in other studies. A technique similar to the present study was used by Jost *et al*[21]; their method involved IMU-assisted implantation of pedicle screws in combination with intraoperative multidimensional visualization and revealed a median offset of 3°. The vertebral rotation of cadaveric specimen was not easy to occur because of its greater weight, whereas spine vertebrae of a lighter minipig was more likely to rotate by continuous loading force. Other techniques like virtual guidance and augmented reality-navigation is also used for assisting pedicle screw insertion.[29,30] A cutoff value of $<5°$ offset between the planned and actual screw trajectories has been proposed[29]; in cases of the exact positioning procedure, the pedicle breach rate during screw placement depended on the tilt deviation of screw trajectory.

The overall detection rate of cortical perforation in the MINS-BIA group was higher than in the FH group. The BIA technique will be helpful for promptly detecting pedicle breach, and thereby the surgeons can adjust the navigator direction to decrease neurovascular injuries. It is worth noting that the positive predictive value in the MINS-BIA group was slightly lower than that of the FH group, which suggested that the predictive ability of a positive detection by BIA technique was not superior to the pedicle feeler probe. After the analysis of postoperative CT images, the results showed that the BIA technique was unable to distinguish cortical perforation of the vertebral body or pedicle breach, resulting in an elevated false-positive rate. Of course, the navigator finder may be positioned more deeply to identify the types of screw

perforation in their future study. Unlike intraoperative neuromonitoring using an electromyographic stimulation probe that a pedicle breach can only be confirmed when the nerve root has been acutely stimulated or damaged,[31,32] BIA provides real-time data on impedance changes, enabling the surgeon to monitor the integrity of the cortical bone and detect cortical bone penetration even when there is no neurologic injury. If this penetration occurs, pedicle drilling should be immediately paused and the forward direction adjusted to reduce the risk of neurovascular complications. This can compensate for the disadvantages of the traditional method of percutaneous pedicle screw fixation, which does not permit the intraoperative use of a general probe.[33,34] Another randomized trial using an electrical pedicle finder to distinguish bone from soft tissue showed that radiation exposure was reduced by 24.5% compared to a standard drilling probe while maintaining 95.9% accuracy.[35] A similar efficacy in detecting perforations by BIA has also been reported in vitro,[36–38] although the same tissue can have different BI values *in vitro* and *in vivo*.

In theory, higher biomechanical stability can be more readily achieved with a larger and longer pedicle screw based on an ideal screw trajectory.[39,40] After a pedicle wall breach, the biomechanical stability of internal fixation will be poor in terms of maximal insertional torque, screw loosening force, axial pullout strength and construct stiffness.[41,42]

Limitations and Directions for Future Research

Although the results obtained with the MINS-BIA–based portable pedicle instrument are encouraging, present study had several limitations. First, the accuracy of the MINS-based technique mainly depends on whether the device has been set to zero before using the pedicle navigator; if this is not done correctly, other electromagnetic instruments and equipment may be affected. Therefore, a hardware/software tool for magnetic compensation is needed to minimize magnetic interference. Additionally, rotation of the spine caused by the loading force of an instrument can alter the initial zero setting, which can be partially compensated by establishing the anatomic relationship between adjacent bony landmarks. Finally, because of variations in bone impedance attributable to environmental and biological factors,[43,44] an animal study may not accurately represent the impedance quality of human bone, especially for patients with osteoporosis; therefore, the clinical applicability of the MINS-BIA–based portable navigator for pedicle screw placement requires validation in a clinical setting.

CONCLUSION

In combination with a 3D CT reconstruction, MINS-BIA assisted implantation of pedicle screw is safe and technically feasible. The animal experiment suggests that this novel pedicle finder could be beneficial for improving or maintaining accuracy while reducing overall radiation exposure, but with no need to change conventional workflow for pedicle screw placement.

➢ Key Points

- ❑ It is still clinically challenging that the pedicle screw malpositioning rate in very difficult spinal surgery ranges from 11.2% to 33%.
- ❑ The planned screw trajectory was more closely matched under micro inertial navigation system than with the free-hand technique in both axial and sagittal planes.
- ❑ The overall detection rate of vertebral cortical perforation by bioelectric impedance analysis was higher than free-hand technique.
- ❑ An animal experiment of twelve minipigs suggested the pedicle finder could be beneficial for improving or maintaining accuracy while reducing overall radiation exposure.

References

1. Boucher HH. A method of spinal fusion. *J Bone Joint Surg Br* 1959;41-B:248–59.
2. Pesenti S, Lafage R, Henry B, et al. Deformity correction in thoracic adolescent idiopathic scoliosis. *Bone Joint J* 2020;102-B:376–82.
3. Kim GU, Yang JH, Chang DG, et al. Effect of direct vertebral rotation in single thoracic adolescent idiopathic scoliosis: better 3-dimensional deformity correction. *World Neurosurg* 2019;129: e401–8.
4. Hojo Y, Ito M, Suda K, et al. A multicenter study on accuracy and complications of freehand placement of cervical pedicle screws under lateral fluoroscopy in different pathological conditions: CT-based evaluation of more than 1,000 screws. *Eur Spine J* 2014;23: 2166–74.
5. Mahesh B, Upendra B, Raghavendra R. Acceptable errors with evaluation of 577 cervical pedicle screw placements. *Eur Spine J* 2020;29:1043–51.
6. Librianto D, Saleh I, Fachrisal, et al. Breach rate analysis of pedicle screw instrumentation using free-hand technique in the surgical correction of adolescent idiopathic scoliosis. *J Orthop Case Rep* 2021;11:38–44.
7. Newell R, Esfandiari H, Anglin C, et al. An intraoperative fluoroscopic method to accurately measure the post-implantation position of pediclescrews. *Int J Comput Assist Radiol Surg* 2018;13:1257–67.
8. Park P. Three-dimensional computed tomography-based spinal navigation in minimally invasive lateral lumbar interbody fusion: feasibility, technique, and initial results. *Neurosurgery* 2015;11 (suppl 2):259–67.
9. Li HM, Zhang RJ, Shen CL. Accuracy of pedicle screw placement and clinical outcomes of robot-assisted technique versus conventional freehand technique in spine surgery from nine randomized controlled trials: a meta-analysis. *Spine (Phila Pa 1976)* 2020;45: E111–9.
10. Caelers I, Rijkers K, van Kuijk S, et al. Neurological events due to pedicle screw malpositioning with lateral fluoroscopy-guided pedicle screw insertion. *J Neurosurg Spine* 2020;1–6.
11. Lyu D, Wang J, He Z, et al. Landmark-based inertial navigation system for autonomous navigation of missile platform. *Sensors (Basel)* 2020;20.
12. Zhang Y, Yu F, Gao W, et al. An improved strapdown inertial navigation system initial alignment algorithm for unmanned vehicles. *Sensors (Basel)* 2018;18.

13. Ribeiro P, Matos AC, Santos PHet al. Machine learning improvements to human motion tracking with IMUs. *Sensors (Basel)* 2020;20:.
14. Sebkhi N, Bhavsar A, Anderson DV, et al. Inertial measurements for tongue motion tracking based on magnetic localization with orientation compensation. *IEEE Sens J* 2021;21:7964–71.
15. Kołodziej M, Ignasiak Z. Changes in the bioelectrical impedance parameters estimating appendicular skeletal muscle mass in healthy older persons. *Aging Clin Exp Res* 2020;32:1939–45.
16. Gertzbein SD, Robbins SE. Accuracy of pedicular screw placement in vivo. *Spine (Phila Pa 1976)* 1990;15:11–4.
17. Senkoylu A, Cetinkaya M, Daldal I, et al. Personalized three-dimensional printing pedicle screw guide innovation for the surgical management of patients with adolescent idiopathic scoliosis. *World Neurosurg* 2020;144:e513–22.
18. Bolger C, Kelleher MO, McEvoy L, et al. Electrical conductivity measurement: a new technique to detect iatrogenic initial pedicle perforation. *Eur Spine J* 2007;16:1919–24.
19. Ahn J, Iqbal A, Manning BT, et al. Minimally invasive lumbar decompression-the surgical learning curve. *Spine J* 2016;16: 909–16.
20. Smith ZA, Fessler RG. Paradigm changes in spine surgery: evolution of minimally invasive techniques. *Nat Rev Neurol* 2012;8:443–50.
21. Jost GF, Walti J, Mariani L, et al. Inertial measurement unit-assisted implantation of pedicle screws in combination with an intraoperative 3-dimensional/2-dimensional visualization of the spine. *Oper Neurosurg (Hagerstown)* 2019;16:326–34.
22. Gokcen HB, Erdogan S, Ozturk S, et al. Sagittal orientation and uniform entry for thoracic pedicle screw placement with free-hand technique: a retrospective study on 382 pedicle screws. *Int J Surg* 2018;51:83–8.
23. Fennell VS, Palejwala S, Skoch J, et al. Freehand thoracic pedicle screw technique using a uniform entry point and sagittal trajectory for all levels: preliminary clinical experience. *J Neurosurg Spine* 2014;21:778–84.
24. Su P, Zhang W, Peng Y, et al. Use of computed tomographic reconstruction to establish the ideal entry point for pedicle screws in idiopathic scoliosis. *Eur Spine J* 2012;21:23–30.
25. Modi HN, Suh SW, Hong JY, et al. Accuracy of thoracic pedicle screw using ideal pedicle entry point in severe scoliosis. *Clin Orthop Relat Res* 2010;468:1830–7.
26. Niswander W, Wang W, Kontson K. Optimization of IMU Sensor Placement for the Measurement of Lower Limb Joint Kinematics. *Sensors (Basel)* 2020;20:.
27. Seel T, Raisch J, Schauer T. IMU-based joint angle measurement for gait analysis. *Sensors (Basel)* 2014;14:6891–9909.
28. Satake K, Kanemura T, Ito K, et al. Pedicle screw placement with use of a navigated surgical drill at subaxial cervical spine. *J Clin Neurosci* 2021;88:28–33.
29. Miller CA, Ledonio CG, Hunt MA, et al. Reliability of the planned pedicle screw trajectory versus the actual pedicle screw trajectory using intra-operative 3D CT and image guidance. *Int J Spine Surg* 2016;10:38.
30. Liebmann F, Roner S, von Atzigen M, et al. Pedicle screw navigation using surface digitization on the Microsoft HoloLens. *Int J Comput Assist Radiol Surg* 2019;14:1157–65.
31. Huang ZF, Chen L, Yang JF, et al. Multimodality intraoperative neuromonitoring in severe thoracic deformity posterior vertebral column resection correction. *World Neurosurg* 2019;127: e416–26.
32. Kim DG, Choi YD, Jin SH, et al. Intraoperative motor-evoked potential disappearance versus amplitude-decrement alarm criteria during cervical spinal surgery: a long-term prognosis. *J Clin Neurol* 2017;13:38–46.
33. Smith ZA, Sugimoto K, Lawton CD, et al. Incidence of lumbar spine pedicle breach after percutaneous screw fixation: a radiographic evaluation of 601 screws in 151 patients. *J Spinal Disord Tech* 2014;27:358–63.
34. Murata K, Fujibayashi S, Otsuki B, et al. Accuracy of fluoroscopic guidance with the coaxial view of the pedicle for percutaneous insertion of lumbar pedicle screws and risk factors for pedicle breach. *J Neurosurg Spine* 2020;1–8.
35. Bai YS, Niu YF, Chen ZQ, et al. Comparison of the pedicle screws placement between electronic conductivity device and normal pedicle finder in posterior surgery of scoliosis. *J Spinal Disord Tech* 2013;26:316–20.
36. Butler RD, Halter RJ. Gauging electrical properties of bone with a bioimpedance-sensing drill. *Physiol Meas* 2019;40:01NT01.
37. Guillen PT, Knopper RG, Kroger J, et al. Independent assessment of a new pedicle probe and its ability to detect pedicle breach: a cadaveric study. *J Neurosurg Spine* 2014;21:821–5.
38. Li Z, Chen C, Lin Y, et al. A novel probe for measuring tissue bioelectrical impedance to enhance pedicle screw placement in spinal surgery. *Am J Transl Res* 2018;10:2205–12.
39. Matsukawa K, Yato Y, Imabayashi H, et al. Biomechanical evaluation of fixation strength among different sizes of pedicle screws using the cortical bone trajectory: what is the ideal screw size for optimal fixation. *Acta Neurochir (Wien)* 2016;158:465–71.
40. Matsukawa K, Yato Y, Imabayashi H. Impact of screw diameter and length on pedicle screw fixation strength in osteoporotic vertebrae: afinite element analysis. *Asian Spine J* 2020;15:566–74.
41. Calvert GC, Lawrence BD, Abtahi AM, et al. Cortical screws used to rescue failed lumbar pedicle screw construct: a biomechanical analysis. *J Neurosurg Spine* 2015;22:166–72.
42. Stauff MP, Freedman BA, Kim JH, et al. The effect of pedicle screw redirection after lateral wall breach–a biomechanical study using human lumbar vertebrae. *Spine J* 2014;14:98–103.
43. Bhardwaj P, Rai DV, Garg ML, et al. Potential of electrical impedance spectroscopy to differentiate between healthy and osteopenic bone. *Clin Biomech (Bristol, Avon)* 2018;57:81–8.
44. Koury JC, de Oliveira-Junior AV, Portugal M, et al. Bioimpedance parameters in adolescent athletes in relation to bone maturity and biochemical zinc indices. *J Trace Elem Med Biol* 2018; 46:26–33.